



Research paper

Insight into imiquimod skin permeation and increased delivery using microneedle pre-treatment

Mohammed Hussain Al-Mayahy^{a,b}, Akmal H. Sabri^a, Catrin S. Rutland^c, Amy Holmes^d, John McKenna^e, Maria Marlow^a, David J. Scurr^{a,*}

^a Division of Advanced Materials and Healthcare Technologies, School of Pharmacy, The University of Nottingham, NG7 2RD, UK

^b Pharmaceutics Department, College of Pharmacy, Mustansiriyah University, Baghdad, Iraq

^c School of Veterinary Medicine and Science, The University of Nottingham, NG7 2RD, UK

^d School of Pharmacy and Medical Sciences, University of South Australia, Adelaide, Australia

^e Department of Dermatology, University Hospitals of Leicester, Leicester Royal Infirmary, Leicester, UK



ARTICLE INFO

Keywords:

Time-of-flight secondary ion mass spectrometry

Microneedles

Basal cell carcinoma

Imiquimod

Permeation enhancer

ABSTRACT

Basal cell carcinoma (BCC) is the most common skin cancer in humans. Topical treatment with imiquimod provides a non-invasive, self-administered treatment with relatively low treatment cost. Despite displaying excellent efficacy, imiquimod is only licensed by the FDA for superficial BCC. The current work employed HPLC and ToF-SIMS analysis to provide a novel assessment of imiquimod permeation from Aldara™ cream in skin depth and lateral distribution. Using Aldara™ cream and *in vitro* Franz cell studies with subsequent HPLC analysis, it is apparent that most of the topically applied imiquimod cream is left on the skin surface with more than 80% of the drug being recovered from skin wash. In addition, ToF-SIMS chemical imaging of recovered tape stripped skin samples illustrated significant detection of imiquimod signal over the entire skin area for the upper tape strips, whereas the deeper strips show large portions of the skin area without detected imiquimod. Given the limited permeation depth and non-uniform permeation observed at tape strips 6–18 when applied as a topical imiquimod cream, a permeation enhancement strategy utilising a skin pre-treatment with a microneedle device was investigated as a method to improve intradermal delivery. The recovered amount of imiquimod in tape strips and remaining skin determined by HPLC was approximately three times higher when Aldara™ was applied on microneedle pre-treated skin relative to intact skin. The ToF-SIMS ion images of the tape strips and cross-sections illustrated the existence of imiquimod in the microchannels which then laterally diffuses to peripheral epidermal strata. The current work demonstrates the first known attempt to enhance intradermal delivery of imiquimod using a microneedle device as well as underscoring the complementary role of ToF-SIMS analysis in chemically mapping imiquimod permeation into the skin with high sensitivity.

1. Introduction

Basal cell carcinoma (BCC) is the most common type of skin cancer among Caucasians constituting about 75–80% of skin cancer cases [1]. It has a high prevalence in Europe, Australia and the United States, with approximately 3–4 million cases per year of BCC occur in the United States [2] alone and the incidence rate is rising by 10% annually worldwide [3]. Common aetiologies for BCC are genetic predisposition and exposure to solar radiation (UV light). In addition, increasing age, fair skin with freckles, blond or red hair, blue eyes and male sex represent other risk factors for the condition [4].

The aims of BCC treatment are complete eradication of the tumour with maximum restoration of normal function and acceptable cosmetic

outcome via surgical or non-surgical intervention [5]. Non-surgical approaches include radiotherapy, photodynamic therapy and topical treatment with anticancer drugs such as imiquimod (an immune response modifier with antiviral and antitumor activity) or 5-Fluorouracil (an antimetabolite which inhibits DNA replication in cancer cells). Imiquimod has been demonstrated to be more effective in the treatment of superficial BCC and can be used as the first choice treatment [6].

Surgical excision may not be suitable for some patients because of the invasive nature of the treatment, poor cosmetic outcome, cost and waiting times [4]. Conversely, topical treatment with an anticancer drug such as imiquimod provides a non-invasive, self-administered treatment with excellent cosmetic outcome and lower cost. The four major types of BCC based on morphological classification are superficial

* Corresponding author.

E-mail address: David.Scurr@nottingham.ac.uk (D.J. Scurr).

<https://doi.org/10.1016/j.ejpb.2019.02.006>

Received 7 October 2018; Received in revised form 11 February 2019; Accepted 12 February 2019

Available online 13 February 2019

0939-6411/ © 2019 Published by Elsevier B.V.

(15%), nodular (50%), infiltrative (20%) and mixed (15%) [7]. Several clinical studies have demonstrated the efficacy of imiquimod in the treatment of superficial BCC where cure rates range from 87% to 88% for a 6 week treatment course (once daily/5 days per week), while the cure rates in nodular BCC range from 42% to 76% for a treatment course of 12 weeks (once daily/5 days per week) [8]. As such, the drug is yet to be approved by the FDA for the treatment of nodular BCC. This difference in the clearance rate is attributed to the fact that the lesions in nodular BCC show deeper invasion within the dermis with an inability of imiquimod to permeate through the dermal layer. Several studies have attributed the poor permeation profile of imiquimod within the dermis to its' low water solubility [9]. In addition, the interaction between the amine groups on the drug molecule with the anionic components of the skin may contribute to the poor permeation profile of imiquimod.

Previous studies conducted by Stein et al. [10] and Rehman et al. [11] assessed the permeation of imiquimod into the skin from Aldara™ cream using HPLC. Stein et al. studied the permeation of imiquimod from Aldara™ cream across mouse skin and found that 11.5% of imiquimod from Aldara™ cream permeated across the skin and only 19% remained on the skin surface [10]. Rehman et al. reported a higher amount of imiquimod permeated from Aldara™ cream than from a bigel formulation, where the imiquimod content in the tape strips (TS) from Aldara™ cream was found to be 59.66% of the mean % recovered amount. From both studies imiquimod displayed a high permeability profile from Aldara™ cream into the skin, this can be attributed to the use of mouse skin, since it is thinner and much more permeable than human or pig skin (up to 10 times) [12]. It is also worth noting that in both studies, the researchers employed HPLC to quantify the amount of imiquimod permeated. However, this analysis does not have any imaging capability and therefore it cannot identify the spatial distribution of imiquimod within skin. In the treatment of BCC, uniform distribution is important to ensure complete tumour eradication and hence prevention of future recurrence.

One of the strategies to assist the delivery of topical therapy to deeper BCC is via the use of microneedle technology. Microneedles are arrays of micron-size projections with length ranging between 250 and 1000 µm providing a minimally invasive means to transport drug molecules into and across the skin. They are composed of small micron sized needles which pierce the skin to create microchannels through which drug molecules can be efficiently delivered [13]. In general, microneedles can be characterised into five main groups, namely solid, coated, dissolving, hollow and hydrogel-forming microneedles [14]. These devices confer a minimally invasive and pain-free drug delivery into or across the skin which can improve patient compliance and adherence to treatment. Unlike hypodermic injections, microneedles don't cause bleeding or require trained personnel for administration and can be applied by patients themselves [15].

Microneedles have been used to successfully deliver a range of active pharmaceutical ingredients (APIs) ranging from low molecular weight drugs to macromolecules into and across the skin [15]. Donnelly et al. [16] used a silicon microneedle pre-treatment *in vivo* to enhance skin penetration of 5-ALA into mice skin. They found significantly higher levels of the photosensitiser protoporphyrin IX (PpIX) in the microneedle pre-treated skin compared to intact skin. It is postulated that this microneedle pre-treatment drug delivery approach would be a suitable strategy to improve the delivery of imiquimod into the skin to treat BCC lesions.

Time-of-flight secondary ion mass spectrometry (ToF-SIMS) is a highly sensitive surface analysis technique that can be used to characterise the surface chemistry of a sample. ToF-SIMS exhibits high chemical specificity and provides chemical imaging data [17]. Furthermore, the preparation of samples for ToF-SIMS analysis is relatively simple and does not require an extraction process often used in chromatographic methods or the addition of fluorescent tags or radio-labels [18] except the removal of the excess moisture from the samples prior

the analysis [19]. Judd et al. first used ToF-SIMS to successfully illustrate the permeation of an active agent (chlorhexidine) from 2% w/v aqueous chlorhexidine solution into porcine skin [18]. Sjövall et al. also utilised ToF-SIMS to image the distribution of the active pharmaceutical ingredient (API) 'roflumilast' in mouse skin [20]. In addition, Brunelle and co-workers have conducted considerable work on mapping the permeation profile of fatty acid penetration enhancers into the skin highlighting the utility of ToF-SIMS in tracking the permeation of exogenous compounds into the skin [21–23].

In this study we used an *in vitro* Franz cells with subsequent HPLC and ToF-SIMS analysis to illustrate the permeation depth and lateral distribution characteristics of imiquimod in porcine skin following the application of Aldara™ cream. The same approach was also used to investigate these aspects following a skin pre-treatment using a solid stainless-steel microneedling pen in an attempt to improve the permeation of imiquimod into the skin rendering it more effective in the treatment of deeper nodular type BCC tumours.

2. Materials

Imiquimod was purchased from Bioscience Life Sciences, UK. Aldara™ 5% cream, MEDA Company, Sweden was purchased from Manor pharmacy, UK. A microneedling Dermapen® was purchased from ZJchao, China. Isopentane, HCl, perchloric acid, triethylamine (HPLC grade) and haematoxylin were purchased from Sigma-Aldrich, UK. Acetonitrile (HPLC grade), was obtained from Fisher Scientific, UK. Teepol solution (Multipurpose detergent) was ordered from Scientific Laboratory Supplies, UK. D-Squame standard sampling discs (adhesive discs) were ordered from CUDERM corporation, USA. OCT compound were obtained from VWR International Ltd. Belgium. Deionised water was obtained from an ELGA reservoir, PURELAB® Ultra, ELGA, UK. All reagents were of analytical grade, unless otherwise stated. Gentian violet solution 1% w/v was obtained from De La Cruz products, USA. Porcine skin was used to study the permeation profile of imiquimod due to the limited availability and difficulties associated with the use of *ex vivo* human skin. Nevertheless, various studies have highlighted that porcine skin is a suitable alternative due to the similarities in thickness, histological and permeability properties to human skin [24]. Skin samples were prepared from six month old porcine ears obtained from a local abattoir prior to any cleaning processes. The skin was washed with distilled water and dried using laboratory tissue paper. Hair was carefully cut by scissors to avoid any damage to the *stratum corneum* and the subcutaneous fatty layer was removed using a scalpel. Full skin thickness was used to avoid altering the skin biomechanical properties which may lead to over-penetration of microneedles into the dermal tissue [25]. The full thickness skin samples were then wrapped in aluminium foil and stored at –20 °C. Skin samples were used within six weeks of being frozen. A skin integrity test was performed by measuring the transepithelial electric resistance (TEER) using a modified form of EVOM2 Volt ohmmeter (World Precision Instruments, USA). Skin samples passed the skin integrity test if they showed TEER reading ≥ 3 K Ω [26]. TEER measurements were made prior to performing skin permeation experiments.

3. Methods

3.1. Permeation study of aldara™ cream through porcine skin

Skin samples were mounted on Franz cells with the *stratum corneum* facing upwards. The receptor chamber was filled with 10 mL of 0.1 N HCl used as receptor fluid to keep sink conditions because of the high solubility of imiquimod (basic compound) in this acidic medium 9.5 mg/mL (tested experimentally). Franz cells were then placed in a stirring water bath (Clever Scientific Ltd., UK) at 37 °C for 30 min to equilibrate before applying the formulation. The skin was dosed with 20 mg of Aldara™ cream on infinite dose basis over an area of 0.64 cm².

Infinite dose experiments are defined as experiment where the formulation are applied in a manner that ensures continuous excess of test preparation in the donor compartment. This avoid, the concentration of the drug from being the limiting factor for the permeation of the formulation. Infinite dose is achieved when 100 μL is applied per cm^2 for liquid formulations or 10 mg per cm^2 for solid or semisolid formulation. Such a volume ensures continuous excess of test preparation in the donor compartment [27]. Such dose will produce fundamental permeation behavior and is frequently utilised when testing the drug permeation profile in the presence of permeability enhancers, in this case the permeability enhancement is attributed to the use of microneedles [28]. In order to investigate the utility of microneedles to enhance the permeation profile of imiquimod from commercially available Aldara™ cream, additional Franz cell experiments were performed. However, in this experiment prior to assembling the Franz cells, the skin was placed on a cork support and the microneedle device was applied vertically on the skin. The microneedle device contains 12 solid (metal) micro scale needles of 32 gauge (230 μm diameter). The length of the microneedles used was 250 μm with a minimum speed of vibration of 1000 turn per minute. The application time was kept to 1 min with a mild pressure application (thumb pressure). Thereafter, the skin samples were mounted on Franz cells with the *stratum corneum* facing upwards and followed by the application of the same dose of Aldara™ cream. The receptor fluids for the Franz cells were stirred continuously by a small Teflon-coated magnetic stir bar at 600 rpm and the experiment was ran for 24 h unoccluded. HPLC analysis for imiquimod content from different Franz cells' elements was performed after the 24 h permeation experiment as detailed in Section 3.4.

3.2. Insertion study of microneedles and histological examination of microneedle treated skin

To demonstrate the penetration efficiency of the microneedle device, an insertion and staining protocol with *en face* imaging by a light microscope was followed. Porcine skin was pinned onto a flat cork board to stretch the skin and the microneedling pen was applied vertically on the skin. An electronic microneedle device was used to pierce the skin by vibrational motion of microneedles. These application conditions were used throughout all microneedles experiments. Several drops of gentian violet 1% dye were subsequently applied to cover the treated area and left for 10 min. Afterwards, the excess dye was removed from the skin surface by a tissue towel and Azo wipes (70% v/v IPA, Synergyhealth, UK). The treated skin area was then examined under a light microscope (Leica optical microscope model EC3, Leica Microsystems Ltd., Switzerland) to capture an *en face* image for the microneedle treated skin area.

Following the *en face* imaging of the skin area treated with microneedles by a light microscope, a histological examination was carried out to assess the penetration depth achieved by microneedles. OCT embedding and cryo-sectioning of the skin were performed followed by haematoxylin and eosin staining. Untreated skin samples with microneedles (blank skin) were also subjected to cryo-sectioning, staining and examination under light microscope.

3.3. Tape stripping of porcine skin post-permeation study

After removing the excess cream from the skin surface, the skin was dismantled from the Franz cell assembly and left to air dry at ambient temperature for approximately 2 h. Following this, a tape stripping technique was employed using adhesive tapes (D-Squame, Standard Sampling Discs, USA) with a diameter of 22 mm. The adhesive tapes were applied and removed successively from the same treated skin area for up to 20 strips with the aid of a roller to press the adhesive tape 10 times onto the skin surface to stretch it to avoid the effects of furrows and wrinkles on the tape stripping procedure. A constant speed was used to remove the adhesive tapes from the skin surface by tweezers (in

one swift motion) which were then placed in Eppendorf vials and stored at $-20\text{ }^\circ\text{C}$ until required for analysis [29].

3.4. Measurement of mass balance and HPLC analysis

When the Franz cell experiments were completed (after 24 h), the excess formulation was removed from the surface of the skin by careful application of a combination of very soft dry and moistened sponges with 3% v/v Teepol® detergent solution. The sponges were combined and stored for imiquimod HPLC analysis as a total skin wash. In addition, any cream on the donor chamber inner surface was also removed by the sponges and stored for imiquimod HPLC as a donor chamber wash. The amount of imiquimod from the different Franz cell elements (skin wash, donor chamber wash, pooled tape strips and remaining skin after tape stripping) was extracted by the addition of 20, 10, 5 and 3 mL of methanol extraction mixture (Methanol 90%: Water 9%: 0.1 N HCl 1%) respectively. They were then vortexed for 2 min and left overnight. Following this, they were sonicated for 30 min, filtered through 0.45 μm syringe filter and analysed by HPLC. Receptor fluid samples were filtered through a 0.22 μm centrifuge tube filter and injected directly into the HPLC system without any dilution. HPLC analysis was carried out using an Agilent 1100 series instrument (Agilent Technologies, Germany) equipped with degasser, quaternary pump, column thermostat, autosampler and UV detector. System control and data acquisition were performed using Chemstation software. The details of the HPLC chromatographic conditions are as follows: column C_{18} (150 \times 4.6 mm) ACE3/ACE-HPLC Hichrom Limited, UK. Mobile phase of buffer: acetonitrile (70:30 v/v), the buffer is of 0.005 M sodium 1-octanesulfonate in water containing 0.1% triethylamine adjusted with dilute perchloric acid to pH of 2.2, flow rate of 0.8 mL/minute, UV detection at λ_{max} 226 nm, injection volume of 10 μL and column temperature at 25 $^\circ\text{C}$.

3.5. Cryotome of porcine skin post-permeation study for ToF-SIMS analysis

Skin samples removed from Franz cells were placed in a plastic block containing the optimum cutting temperature (OCT) gel (VWR International Ltd., Belgium) which is an inert mounting medium for cryotomy that solidifies upon rapid cooling. Therefore, the plastic block containing skin immersed in OCT was placed in a beaker of isopentane pre-cooled with liquid nitrogen to solidify. After solidification, the OCT blocks were wrapped in aluminum foil, placed in an airtight plastic bags and stored at $-80\text{ }^\circ\text{C}$. Cryo-sectioning of skin samples were carried out by placing the OCT block in a cryostat chamber (Thermo Cryotome™, UK) at a temperature of $-20\text{ }^\circ\text{C}$. The block was allowed to equilibrate within the cryostat chamber for 30 min and then sectioned using a steel blade into vertical cross sections of 20 μm thickness. Following this, the cryo-sections were mounted onto polysine microscope adhesion slides (ThermoFisher Scientific) and freeze dried for 1 h prior to ToF-SIMS analysis.

3.6. ToF-SIMS analysis

ToF-SIMS was used to analyse individual tape strips and cryo-sectioned skin samples obtained from Franz cell testing. The tape strips and cryo-sectioned skin samples were placed in a freeze dryer for 1 h prior to ToF-SIMS analysis. ToF-SIMS analysis was performed using a ToF-SIMS IV instrument (IONTOF, GmbH) with a Bi_3^+ cluster source. A primary ion energy of 25 KeV was used, the primary ion dose was preserved below 1×10^{12} per cm^2 to ensure static conditions. Pulsed target current of approximately 0.3 pA, and post-acceleration energy of 10 keV were employed throughout sample analysis. The mass resolution for the instrument was 7000 at m/z 28. The area scanned of the tape strips samples was (9 mm \times 9 mm) encompassing the entire skin area exposed to Aldara™ cream during Franz cell diffusion experiments. For the cryo-sectioned skin samples the scanned area was (6 mm \times 6 mm)

or (10 mm × 4 mm) depending on the section size. All the samples were analysed at a resolution of 100 pixels/mm. An ion representing biological material and therefore indicative of skin (skin marker) was identified as CH_4N^+ and was used to threshold the data sets. CH_4N^+ is a common fragment observed in organic materials such as biological specimen. Therefore, this secondary ion was used to track the presence of corneocyte extracted on the tape strips. After that, the data was reconstructed to remove the data from the adhesive tape material found between the fissures in the stripped skin (removing the substrate data) and therefore the data was only analysed from the skin material. Following this, each image of the individual tape strip (9 mm × 9 mm) was divided into four smaller data sets of (4.5 mm × 4.5 mm) which results in four repeats ($n = 4$) for each sample and their intensities were normalised to the total ion intensity. In addition, pure imiquimod and Aldara™ cream reference spectra were obtained by analysing the pure drug and the cream on silicon wafer using ToF-SIMS.

4. Results and discussion

4.1. Measurement of mass balance and HPLC analysis of Aldara permeation from porcine skin

The mean total recovery for mass balance of imiquimod recovered from the different Franz cell components following the permeation study of Aldara™ cream is graphically illustrated in Fig. 1. The recovery percentage of applied dose is highest in the skin wash (90%) as compared to other components indicating that the imiquimod delivered from Aldara™ cream has limited permeation into the skin. A very minor amount (< 1%) was recovered from the remaining skin, suggesting that imiquimod permeation from Aldara™ cream is very limited and is consistent with the FDA approval details and clinical trials that showed the efficacy of Aldara™ cream just for the treatment of superficial BCC lesions [30,31].

The amount of imiquimod observed to permeate in this study is less than that observed by Stein et al. who found 11.5% permeated across the skin from Aldara™ cream and only 19% remained on the skin

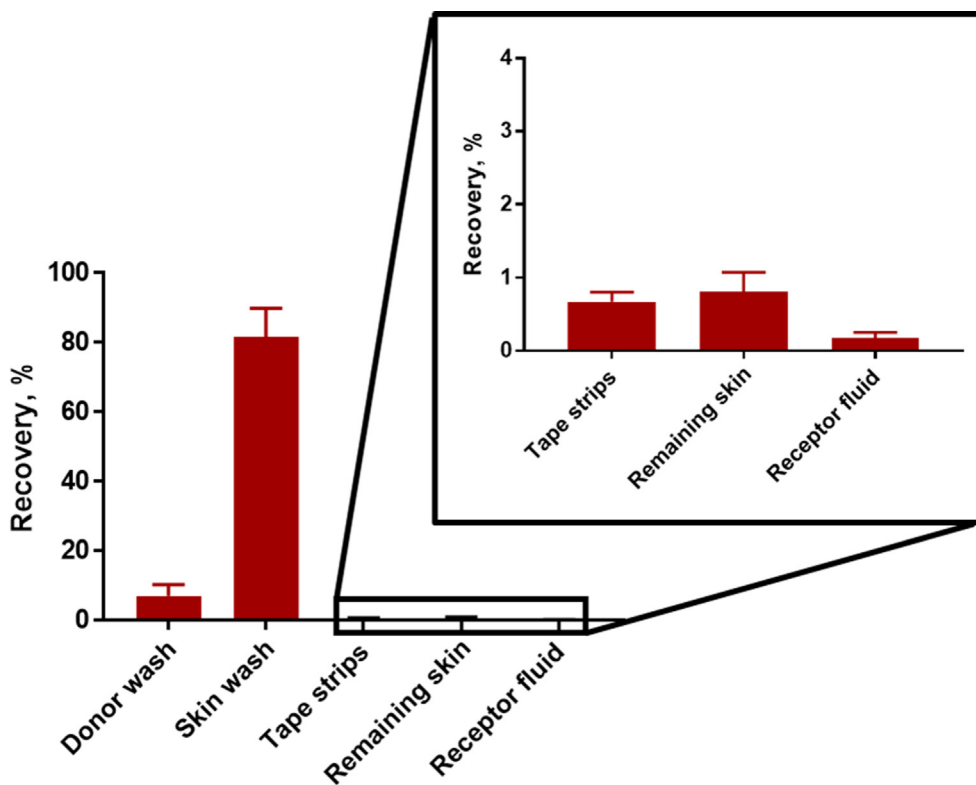


Fig. 1. Mean total recovery for mass balance of applied dose amount of imiquimod from the different Franz cell components (donor chamber wash, skin wash, tape strips, remaining skin and receptor fluid) of the permeation study of Aldara™ cream when analysed by HPLC. Data is presented as the mean \pm SD ($n = 6$). The inset provides details on the amount of imiquimod that have permeated into (tape strips and remaining skin) and across (receptor fluid) the skin.

surface when analysed by HPLC [10]. This higher imiquimod permeability observed by Stein et al. can be attributed to the use of mouse skin, since it is thinner and much more permeable than human or pig skin (up to 10 times) [32,33].

The high lipophilicity and low aqueous solubility of imiquimod suggests that it may have easier permeation into the *stratum corneum* layer compared with the more aqueous viable epidermis and therefore it may form a depot within the *stratum corneum* since the viable epidermis has a high-water content. Several studies have shown that lipophilic drugs and lipophilic UV filters tend to be preferably located or accumulated on the skin surface and in the superficial layers of the *stratum corneum* [34,35]. Using porcine skin, as a suitable alternative to human skin, the current results are in agreement with these findings and highlight the superficial permeation of imiquimod into the skin. Such findings further corroborate the licensing restriction imposed by the FDA on Aldara™ cream for the treatment of superficial BCC over the nodular variants. Although the HPLC analysis provides useful quantitative results, the analytical technique does not confer any detail regarding imiquimod distribution within individual layers of skin. Therefore, additional analytical techniques were explored in an attempt to provide such spatial detail regarding imiquimod permeation.

4.2. ToF-SIMS analysis of tape strips post permeation study

Due to the several advantages offered by ToF-SIMS outlined in Judd et al. [18], this technique was implemented in this study to glean a more detailed insight into permeation of imiquimod from Aldara™ cream including an analysis of individual tape strips and imaging of the chemical distribution of imiquimod at their surface. Prior to ToF-SIMS analysis of the tape strips, some preliminary ToF-SIMS experiments were performed to obtain reference spectra of pure imiquimod and Aldara™ cream. ToF-SIMS survey spectra of pure imiquimod and Aldara™ cream reference on silicon wafer in positive polarity are shown in Fig. 2(a) and (b) respectively.

As shown in Fig. 2(a), two secondary ion peaks relevant to imiquimod are observed in the positive polarity spectra, the molecular ion

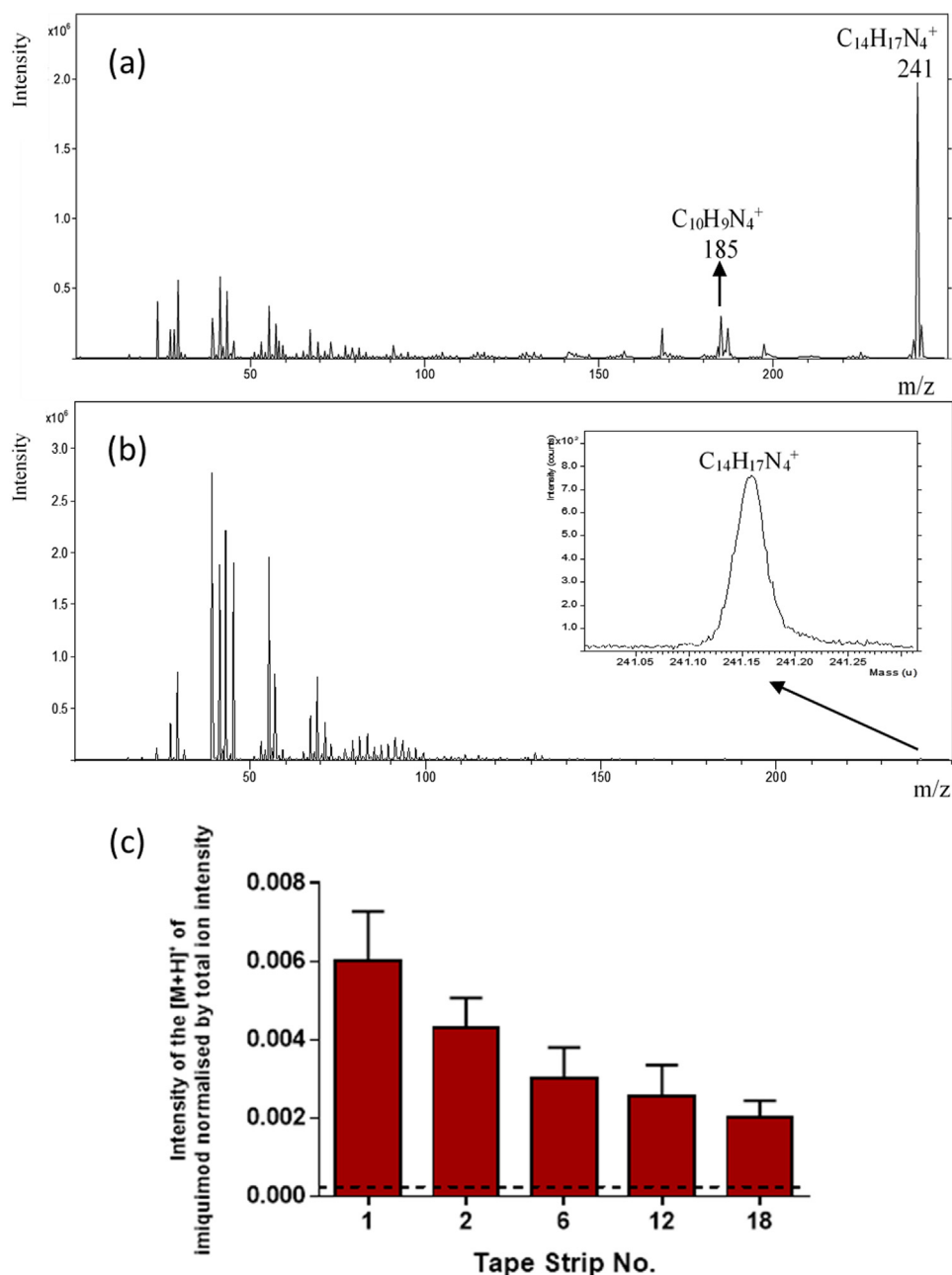


Fig. 2. Positive polarity ToF-SIMS survey spectra of (A) imiquimod reference and (b) Aldara™ cream, where the inset spectrum shows the peak of the [M+H]⁺ of imiquimod at $m/z = 241$. (c) Ion intensity values of the [M+H]⁺ of imiquimod in Aldara™ cream tape strips normalised by total ion intensity. Data is presented as the mean \pm SD ($n = 4$). The dotted black line represents the ion intensity obtained from the control skin samples.

[M+H]⁺ peak of imiquimod C₁₄H₁₇N₄⁺ ($m/z = 241$) and the fragment ion peak C₁₀H₉N₄⁺ ($m/z = 185$). The [M+H]⁺ of imiquimod C₁₄H₁₇N₄⁺ which resulted from the ionisation of the whole imiquimod molecule C₁₄H₁₆N₄ (M.wt. 240) is more intense than the fragment ion peak. In the negative polarity only a fragment ion peak, C₁₀H₈N₄⁻ ($m/z = 184$), is observed (Supporting Information, Fig. S1). The positive polarity data is therefore considered to be more informative than the negative polarity due to the presence of the [M+H]⁺ at a relatively high intensity which provides unambiguous identification of imiquimod. Therefore, the ToF-SIMS data of imiquimod will be presented in the positive mode only.

The ToF-SIMS survey spectrum of Aldara™ cream is shown in Fig. 2(b). Although the peak of the [M+H]⁺ of imiquimod in Aldara™ cream is not as intense as observed for the pure imiquimod reference material Fig. 2(a), it is clearly resolved suggesting that ToF-SIMS can be

used to identify imiquimod in Aldara™ cream.

To assess the exact permeation of imiquimod and to visualise its distribution within the *stratum corneum*, tape strips obtained from Franz cell experiments were analysed by ToF-SIMS. The secondary ion intensity data for the [M+H]⁺ ion of imiquimod in Aldara™ cream treated skin tape strips are shown in Fig. 2(c) whereby it can be observed that this ion is observed above the control intensity throughout the series of 18 tape strips (therefore approximately illustrating the full depth of the *stratum corneum*). A decreasing ion intensity is observed from the outer surface of the skin (TS 1) to the inner layers of the *stratum corneum* (TS 18). The ability of the ToF-SIMS to analyse single tape stripped skin samples (layer by layer of skin analysis) to map the permeation of imiquimod within the *stratum corneum* has not been previously observed and this study provides further insight into the exact depth of permeation achieved with this drug. This decreasing

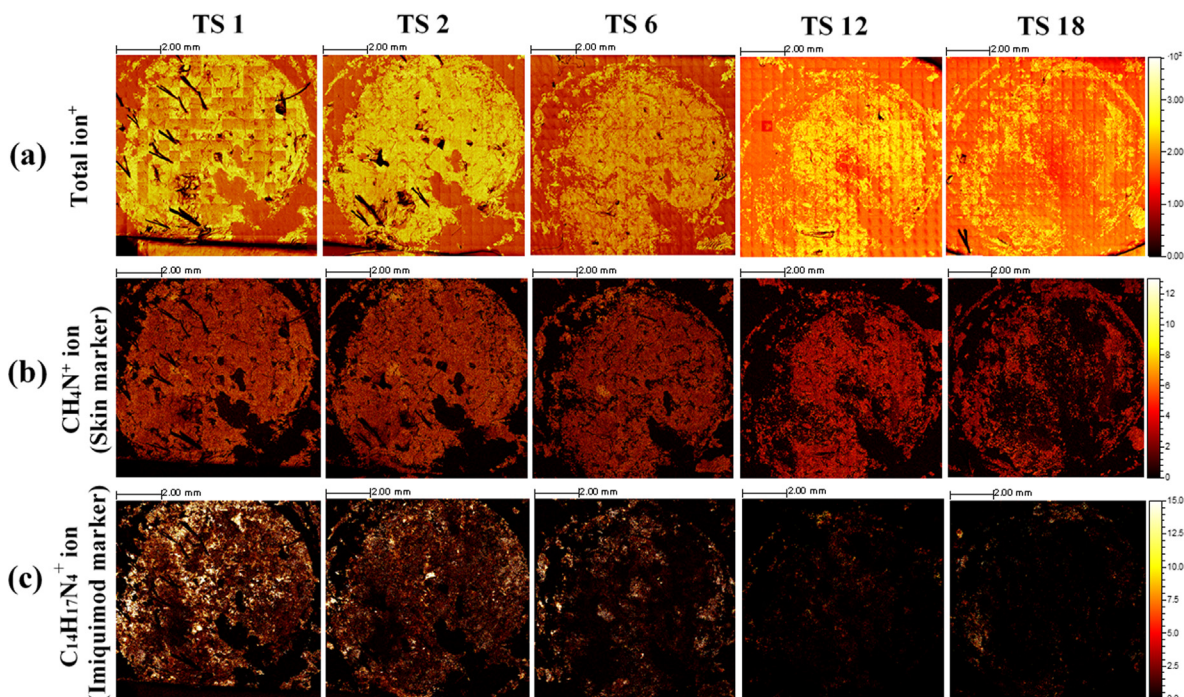


Fig. 3. ToF-SIMS ion images of Aldara™ cream treated skin tape strips showing the (a) the total (b) skin marker (CH_4N^+) and (c) imiquimod marker ($\text{C}_{14}\text{H}_{17}\text{N}_4^+$) ions. The scanned area is (9 mm × 9 mm).

permeation of imiquimod at the inner layers of the *stratum corneum* is consistent with the HPLC results that demonstrated a limited permeation of imiquimod into the deeper skin layers (less than 1% recovered from the remaining skin specimen).

ToF-SIMS ion images of the entire tape stripped area, which represents the whole exposed area of the skin to Aldara™ cream during Franz cell diffusion experiment (9 mm diameter), are illustrated in Fig. 3. The total, skin marker (CH_4N^+), and imiquimod marker ($\text{C}_{14}\text{H}_{17}\text{N}_4^+$) ion images are shown in Fig. 3(a)–(c) respectively. The intensities are scaled to the same value to enable a valid or fair comparison.

An examination of the skin marker, CH_4N^+ (Fig. 3(b)), shows that the amount of skin (corneocytes) attached per tape strip is reduced moving from the outer skin surface (TS 1) towards the inner layers of the *stratum corneum* (TS 18). Although there is some reduction, the significant reduction appears to occur at around TS 12 and that TS 1, 2 and 6 show a large amount of stripped corneocytes. This would be anticipated and similar observations of decreasing skin amount from the upper to lower tape strips have been reported by other studies when corneocytes on tape strips were determined by different methods such as the weighing method, protein assay method and UV/visible method. This is due to the increased cohesion between the cells at the deeper *stratum corneum* layers compared to the outer layers which results in reduced amounts of skin being removed by a tape strip [36–38].

The ion images of the $[\text{M}+\text{H}]^+$ of imiquimod (Fig. 3(c)) are observed to decrease from the uppermost layer (TS 1) towards the deeper layer of the *stratum corneum* (TS 18) correlating with the ion intensity data shown in Fig. 2(c). Although TS 1 and 2 show a non-uniform distribution of the $\text{M}+\text{H}^+$ ion, there are very few instances where the $\text{M}+\text{H}^+$ ion is not present coincident with the skin marker. This suggests that within the first two layers of skin the imiquimod has permeated significantly and would potentially explain its ability to successfully treat superficial BCC tumours. The skin marker for TS 6 shows some reduction in the amount of skin removed but nonetheless still shows most of the Franz cell area. The ion distributions within TS 6 exhibit some areas where the $\text{M}+\text{H}^+$ for imiquimod and the skin marker do not correlate, where the $\text{M}+\text{H}^+$ for imiquimod is absent. It is proposed

that although imiquimod has permeated to this layer of the skin, it has not done so uniformly with absent patches up to several millimetres in diameter. It is evident from the skin marker ion that TS 12 and 18 exhibits significantly less skin than previous strips, however, it is clear that relatively little of the $\text{M}+\text{H}^+$ ion of imiquimod can be observed correlating with the location of the skin. It is proposed that some imiquimod has permeated to the lower region of the *stratum corneum*, however, it has done so in very small areas often no larger than 1 mm in diameter.

This observed non-uniform distribution of imiquimod within skin from TS 6 onwards can decrease the efficacy of Aldara™ cream to effectively treat whole BCC lesions. The pattern of drug distribution within the skin layers is very important in BCC because the whole lesion area should be treated evenly at the effective concentration to ensure complete cure and prevent recurrence. Therefore, the ability to assess this is of great importance, since the topical treatment of BCC lesions with Aldara™ cream has shown higher recurrence rate in comparison to surgery [8], particularly tumours with thickness > 0.4 mm [39]. These findings show detailed permeation of imiquimod down to TS 18. The non-uniformity in later layers supports the rationale of why FDA restrict the license of Aldara™ for the treatment of superficial BCC over nodular BCC.

4.3. Insertion study of microneedles and histological examination of microneedle treated skin

Given the limited permeation profile of imiquimod when applied as a topical cream, the utility of a skin pre-treatment using a microneedle pen as a permeation enhancement strategy was pursued. However, prior to this, the insertion profile of the device was investigated. An image of the 12-metal microneedle cartridge that is fixed in the microneedle device is shown in Fig. 4(a). The diameter of the base (circular shape) containing the 12 microneedles is 5 mm and the distance between each microneedle pin is approximately 1.5 mm.

To demonstrate the efficiency of the microneedle device to penetrate the uppermost layer of the skin, *en face* imaging by light microscopy was performed for the porcine skin samples treated with the

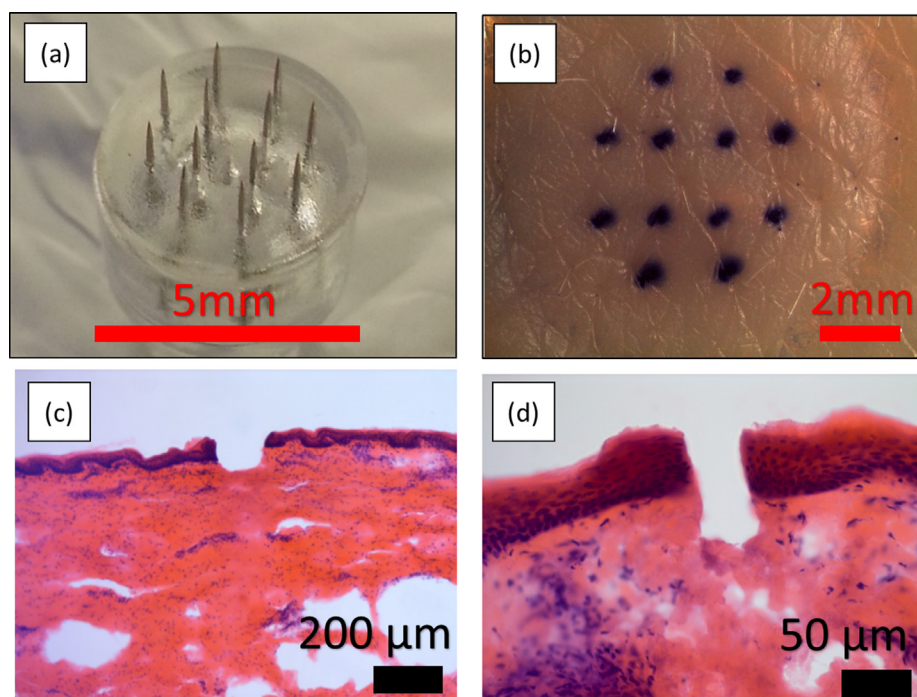


Fig. 4. En face images of (a) the microneedles cartridge fixed in the microneedle device used to pierce the skin, (b) porcine skin following microneedle device treatment and staining with gentian violet. (c) Light microscope images H&E stained cross-sections identifying the location of the microchannels within skin tissue (d) H&E stained cross-sections but at a higher magnification.

microneedles and stained with gentian violet as illustrated in Fig. 4(b). These images show that the dyes are appropriately retained in the microchannels formed by the microneedles. This indicates the capability of the microneedles to successfully pierce the skin.

The microneedling device penetration efficiency was observed to occur in a reproducible manner throughout the tested skin samples which can be attributed to the fixed velocity used in the microneedles insertion provided by the microneedle device. Verbaan et al. demonstrated that the use of an electrical applicator for microneedles with 300 μm length at certain velocity facilitates the insertion of the microneedles into the skin in a reproducible manner compared to manual application [40]. The stained cross-sections with H&E highlight the location of the microchannels within skin tissue and it can be observed that the microneedles penetrate the *stratum corneum* and viable epidermis to reach the papillary dermis (PD) layer (the layer located directly beneath the viable epidermis). In order to measure the pore size, the diameter of the stained pores could be measured to provide an estimate of the size of the microchannels formed. However, as diffusion may occur, a more accurate way to estimate the pores diameter is to cryo-section the skin samples directly following insertion and measure the channel diameter via microscopy. It can be seen from Fig. 4b that the measured diameter of the pores ranged from 300 to 500 μm . However, these values are in contrast to the measured values from the cryo-sectioned samples (Fig. 4c and d) that showed the diameter of the pores to be between 40 and 95 μm . This overestimation of the pore size is thought to be due to the lateral diffusion of the dyes to the surrounding dermal tissue. An apparent limitation of the *en face* imaging method of visualising microneedles treated skin is the overestimation of the pore diameter because of the lateral diffusion of the dyes [41,42]. In addition, a recent study conducted by Coulman et al. highlighted that such overestimation may also arise from tissue processing steps which influence tissue hydration and elasticity of the skin [42]. However, such overestimation will not affect the goal of the study which is to use the microneedling pen to breach the *stratum corneum* in order to generate conduits to promote the delivery of imiquimod into the skin. A noteworthy point is that the microneedle cartridge fixed to microneedle device is disposable and can be used just for one application and then replaced with a new one for the next sample. This diminishes any damage that may occur to the integrity of microneedles from repeated

applications and increases the microneedles penetration reproducibility. Simultaneously, from the clinical perspective this eliminates any safety issue generated from the breaking of the microneedles within skin from the reuse of the same microneedles.

4.4. Mass balance measurement and HPLC analysis of imiquimod from Aldara™ application on microneedle pre-treated skin

The mean percentage recovered amounts of imiquimod from the different Franz cell elements of the permeation study of Aldara™ cream with and without microneedles pre-treatment are reported in Table 1. It is observed in Table 1 that the mean percentage recovered amount of imiquimod from tape strips and remaining skin elements of Aldara™ cream with microneedles pre-treatment is approximately three times higher than the Aldara™ cream alone. This provides a greater opportunity for the cream to more efficiently treat whole superficial or nodular BCC lesions. In addition, the statistical comparison between the recovered amounts of imiquimod in the remaining skin shows that the recovered amount of imiquimod with microneedle pre-treatment is significantly higher (Unpaired Student's *t*-test $p < 0.05$) than the Aldara™ cream alone as illustrated in Fig. 5.

Furthermore, it is observed that with microneedle pre-treatment the imiquimod's amount in the receptor fluid is approximately ten times higher than the Aldara™ cream alone. This increase in the recovered amount of imiquimod in the receptor fluid is perhaps anticipated since

Table 1

Mean percentage recovered amount of imiquimod from the different Franz cell elements of the permeation study of Aldara™ cream with and without microneedle pre-treatment when analysed by HPLC. Data is presented as the mean $\% \pm \text{SD}$ ($n = 6$).

Analysed element	Aldara™ cream only (mean % recovery \pm SD)	Aldara™ cream with microneedles pre-treatment (mean % recovery \pm SD)
Donor wash	7.11 \pm 3.27	9.38 \pm 4.59
Skin wash	81.72 \pm 8.14	72.39 \pm 12.02
Tape strips	0.67 \pm 0.13	2.38 \pm 2.40
Remaining skin	0.81 \pm 0.26	2.27 \pm 0.39
Receptor fluid	0.17 \pm 0.08	1.89 \pm 0.47

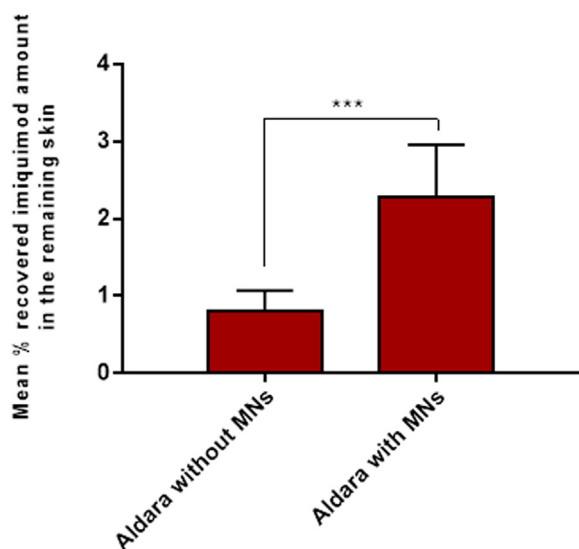


Fig. 5. Mean percentage recovered imiquimod amount in the remaining skin of the permeation study of Aldara™ cream with and without microneedle pre-treatment when analysed by HPLC. Data is presented as the mean \pm SD (n = 6). Unpaired Student's *t*-test $p < 0.05$.

the microchannels created by microneedles can reach the depth of the papillary dermis layer and thus higher amounts of imiquimod bypass the skin barriers and are presented in the receptor fluid. For *in vivo* conditions, this would suggest that higher amounts of imiquimod would be available for systemic circulation which may lead to increase the risk of imiquimod's systemic adverse effects. However, in BCC patients the *stratum corneum* becomes thicker because of the hyperkeratinisation associated with the tumour lesions [30] and the microchannels created by microneedle device may not reach the depth of papillary dermis and hence less amounts of imiquimod would be available for systemic absorption. Besides that, it could be argued that the utilisation of such device may push cancerous cells from superficial BCC into the dermis leading to the potential risk of seeding and spreading the cancer cell in a new dermal microenvironment. However, the propensity for such phenomenon is minimal due to the nature of BCC cells which is highly dependent on its microenvironment for survival [43]. However, in an attempt to limit the likelihood of such side effect, the use microneedle device could be reserved only for deeper BCC lesions such as those seen in nodular and infiltrative BCC.

4.5. ToF-SIMS analysis of tape strips from skin pre-treated with microneedles and subsequent Aldara™ cream application

ToF-SIMS analysis of the tape strips of Aldara™ cream on microneedle pre-treated skin shows a significant increase in the ion intensity of the $[M+H]^+$ of imiquimod in tape strips 2, 5 and 10 compared to the Aldara™ cream alone, as shown in Fig. 6(a). This indicates that a higher amount of imiquimod had permeated into the *stratum corneum* following the microneedle application which is in accordance with the HPLC results (Table 1).

ToF-SIMS ion images of tape strip two of Aldara™ cream with microneedle pre-treatment are shown in Fig. 6(b). It can be seen that the pattern of imiquimod distribution follows the pattern of the microneedle array on the device (Fig. 4(a)). In addition, imiquimod is mostly localised in the area disrupted by the application of the microneedle device (i.e. at a circular region in the middle of the tape strip which corresponds to the shape of the microneedle device cartridge). Fig. 6(b) also shows that imiquimod ion, highlighted in green, laterally diffuses out of the microchannels and distributes to the peripheral epidermal tissue. Such findings indicate that the utilisation of microneedling pen in tandem with Aldara™ cream application is able to promote lateral

permeation of drug to surrounding skin tissues. Such apparent lateral permeations have been observed by various groups using conventional techniques such as fluorescent microscopy. These groups have attributed that the observed lateral permeation is due to the overlapping drug diffusion fronts from individual microneedle sites [44,45]. However, there is yet any research to date that have observed enhancement in lateral permeation using ToF-SIMS.

4.6. ToF-SIMS analysis of skin cross-sections

ToF-SIMS analysis of cryo-sectioned skin samples were used to map imiquimod permeation within different skin layers. Skin cross-sectioning can be used as a complementary tool to the tape stripping technique to follow and visualise drug permeation within skin. ToF-SIMS analysis of the cryo-sectioned skin samples shows that the ion intensity of the $[M+H]^+$ imiquimod from Aldara™ cream with microneedle pre-treatment is significantly higher than the ion intensity obtained from the samples without microneedle pre-treatment as shown from their overlaid spectra (Supporting Information Fig. S2). This corresponds with the data obtained by tape stripping shown in Fig. 6(a). It is thought with the presence of the microchannels created by the microneedles, imiquimod penetration is not only restricted to the microchannel site but it radiates to the adjacent tissue (lateral distribution as observed in Fig. 6(b)) which results in almost continuous higher intensity zones of imiquimod localised at the upper skin strata.

The ToF-SIMS ion images of the cryo-sectioned skin samples of Aldara™ cream with microneedle pre-treatment are illustrated in Fig. 7 which show the total and the overlay image of the skin marker, CH_4N^+ with imiquimod molecular ion $C_{14}H_{17}N_4^+$ (Fig. 7a and b respectively). An examination of the total ion image and the skin marker image indicates the location of the microchannels within the skin sections (white arrows in Fig. 7(a) and (b)) created by the application of microneedles. The $[M+H]^+$ imiquimod ion image shown in the overlay image (Fig. 7(b)) highlights the distribution of imiquimod at the upper layer of the skin sections in addition to its localisation in the microchannels. It is apparent that there are some indentations in the skin that may have formed upon microneedle application. However, not the entire top layer of the cross-section contains such indentations despite the entire section of the skin analysed covers the entire microneedle treated region. This may be due to the viscoelastic nature of the skin that causes some regions of the skin to recoil and recover over time from the indentations formed from microneedle application.

For evaluating the difference between the two treatments in Fig. 7(b), it is worth highlighting that the imiquimod signal arising from the *stratum corneum* is of great interest for the comparison. From Fig. 7 it is evident that there is limited availability of imiquimod within the skin layers when applied as a topical cream alone. However, when Aldara™ is applied to the microneedle pre-treated skin, we can observe that imiquimod is mostly located in the *stratum corneum* which makes imiquimod available in this layer. Such an observation would suggest lateral permeation of imiquimod following cream application on microneedle treated skin which further supports the results illustrated in Fig. 6. It is clear here that the imaging capability of ToF-SIMS illustrates where the drug is localised within the skin tissues. Such findings may be of heuristic value in guiding the development of such systems in order to improve intradermal delivery of therapeutics. However, we are unable to see imiquimod in deeper layers using cross-sections as the drug is diluted over a wide area of the dermis and epidermis. In comparison, the HPLC data from Table 1 suggests increased intradermal delivery with microneedle skin pre-treatment. Such imiquimod detection was achieved as the extraction procedure concentrates imiquimod from the remaining skin allowing detection with the HPLC instrument.

The HPLC and ToF-SIMS results of Aldara™ cream with microneedle pre-treatment quantitatively and qualitatively demonstrate increased delivery of imiquimod into the epidermal skin layers and suggest its potential usefulness for more efficient treatment of both superficial and

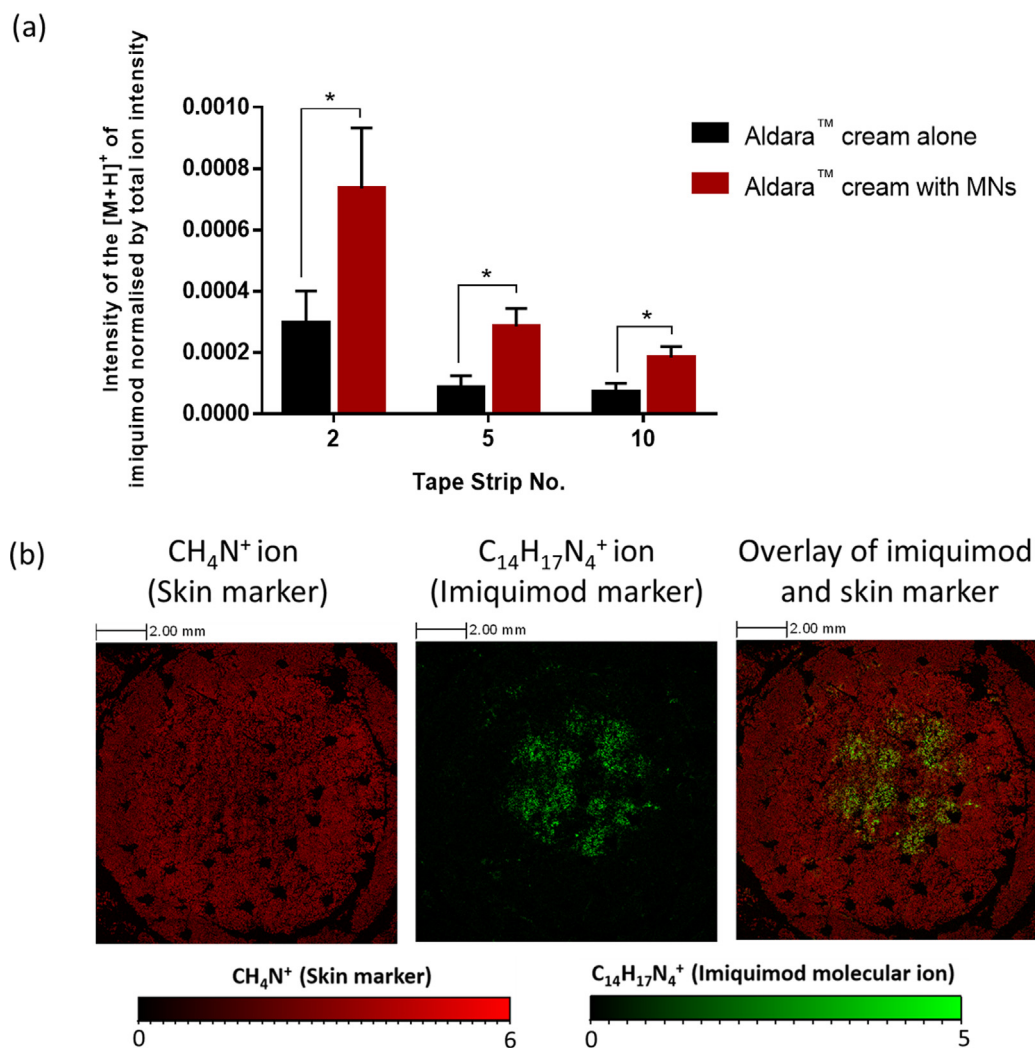


Fig. 6. a) Ion intensity values of the $[M+H]^+$ of imiquimod ($C_{14}H_{17}N_4^+$) in Aldara™ cream tape strips (2, 5 and 10) with and without microneedle pre-treatment normalised by total ion intensity. Data is presented as the mean \pm SD ($n = 4$). Unpaired Student's t -test $p < 0.05$ (b) ToF-SIMS ion images of tape strip two of Aldara™ cream with microneedles pre-treatment showing: the skin marker (CH_4N^+), the imiquimod marker ($C_{14}H_{17}N_4^+$), and the overlaid image of imiquimod (green colour) and the skin (red colour). The scanned tape strip area is of $12 \times 12 \text{ mm}^2$.

nodular BCC lesions. In addition, both the Aldara™ cream and the microneedle device are commercially available systems making them easily accessible. This study is considered to be a proof-of-concept analysis providing an insight into the potential use of microneedles for improving imiquimod's skin penetration and further *ex vivo* and *in vivo* investigation on human skin with BCC lesions are required to optimise the final application conditions.

5. Conclusions

The current work demonstrates a novel application of Franz diffusion cells, skin tape stripping and skin cryo-sectioning with subsequent analysis by HPLC and ToF-SIMS to map and visualise the distribution of imiquimod into the skin from the commercial product Aldara™. The ToF-SIMS ion images of Aldara™ cream tape strips illustrated a non-uniform distribution of imiquimod within deeper skin strata which is consistent with the FDA approval and clinical trials for the treatment of superficial BCC. In addition, this study also highlights the potential advantages of solid microneedle skin pre-treatment in conjunction with Aldara™ cream application to enhance the delivery of imiquimod into the epidermal layers of the skin for the treatment of the deeper and more invasive nodular BCC lesions. This work also demonstrates the heuristic value and complementary role of the ToF-SIMS technique in

the analysis and imaging of imiquimod permeation into the skin with high sensitivity and chemical specificity without the need of fluorescent tags or radiolabels.

Acknowledgements

The authors would like to thank Mustansiriyah University (www.uomustansiriyah.edu.iq) Baghdad-Iraq for its support in the present work. This work was also supported by the Engineering and Physical Sciences Research Council (EPSRC) [grant number: EP/L01646X/1] via a PhD sponsorship for Akmal Sabri; at the Centre for Doctoral Training for Advanced Therapeutics and Nanomedicine at the University of Nottingham. We would like to thank Dr. Mark Prausnitz from Georgia Tech School of Chemical and Biomolecular Engineering for his insightful discussion and advice provided on the use of gentian violet to locate microneedle channels.

Conflict of interest

None.

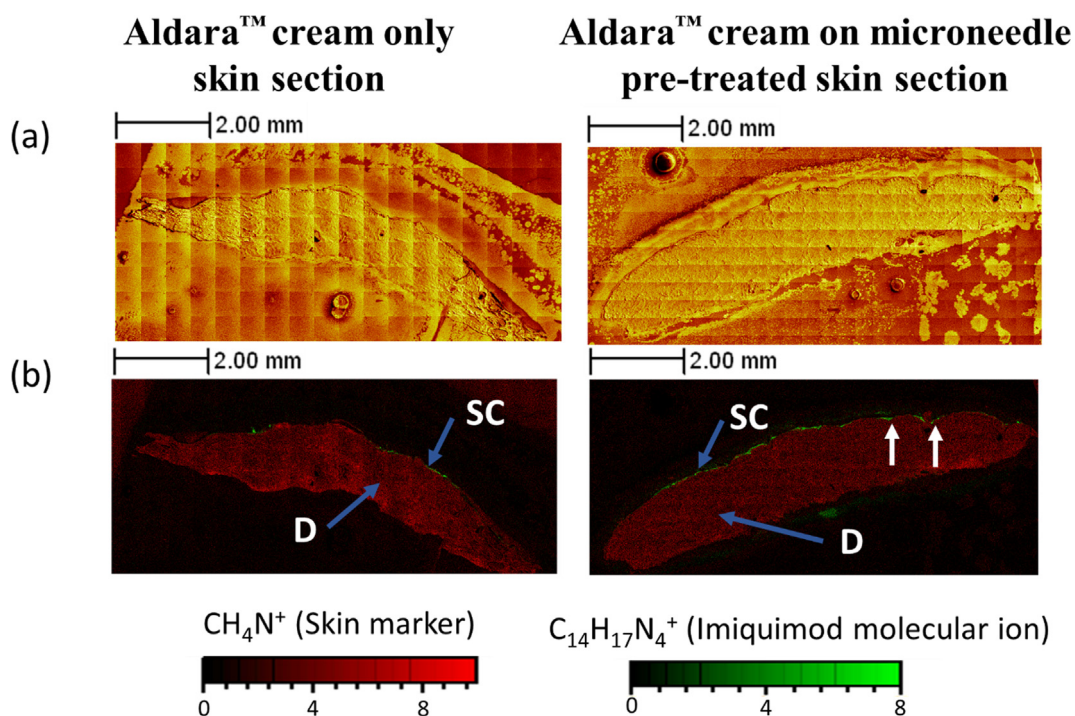


Fig. 7. ToF-SIMS ion distribution map of porcine skin cross sections from Aldara™ cream on intact skin and microneedles pre-treated skin. (a) the total ion⁺, (b) an overlay image of the skin marker (CH_4N^+) with imiquimod marker ($\text{C}_{14}\text{H}_{17}\text{N}_4^+$) to indicate the localisation of imiquimod within the *stratum corneum*. SC indicates *stratum corneum*, D indicates dermis. White arrows indicate microneedle indentation into the skin that still persist after 24 h. The skin cross-section covers the microneedle-treated part of the skin as the microneedle array is 5 mm wide.

Appendix A. Supplementary material

Supplementary data to this article can be found online at <https://doi.org/10.1016/j.ejpb.2019.02.006>.

References

- [1] T.L. Diepgen, V. Mahler, The epidemiology of skin cancer (accessed August 18, 2018), *Br. J. Dermatol.* 146 (Suppl 61) (2002) 1–6 <http://www.ncbi.nlm.nih.gov/pubmed/11966724>.
- [2] M. Alam, L.H. Goldberg, S. Silapunt, E.S. Gardner, S.S. Strom, A.W. Rademaker, D.J. Margolis, Delayed treatment and continued growth of nonmelanoma skin cancer, *J. Am. Acad. Dermatol.* 64 (2011) 839–848, <https://doi.org/10.1016/j.jaad.2010.06.028>.
- [3] V. Madan, J.T. Lear, R.-M. Szeimies, Non-melanoma skin cancer, *Lancet* 375 (2010) 673–685, [https://doi.org/10.1016/S0140-6736\(09\)61196-X](https://doi.org/10.1016/S0140-6736(09)61196-X).
- [4] N.R. Telfer, G.B. Colver, C.A. Morton, British Association of Dermatologists, Guidelines for the management of basal cell carcinoma, *Br. J. Dermatol.* 159 (2008) 35–48, <https://doi.org/10.1111/j.1365-2133.2008.08666.x>.
- [5] G. Goldenberg, L.E. Golitz, J. Fitzpatrick, *Histopathology of skin cancer*, in: *Manag. Ski. Cancer*, Springer Berlin Heidelberg, Berlin, Heidelberg, 2010, pp. 17–35. doi: 10.1007/978-3-540-79347-2_2.
- [6] A.H. Aris, K. Mosterd, B.A. Essers, E. Spoorenberg, A. Sommer, M.J. De Rooij, H.P. van Pelt, P.J. Quaedvlieg, G.A. Krekels, P.A. van Neer, J.J. Rijzewijk, A.J. van Geest, P.M. Steijnen, P.J. Nelemans, N.W. Kellens-Smeets, Photodynamic therapy versus topical imiquimod versus topical fluorouracil for treatment of superficial basal-cell carcinoma: a single blind, non-inferiority, randomised controlled trial, *Lancet Oncol.* 14 (2013) 647–654, [https://doi.org/10.1016/S1470-2045\(13\)70143-8](https://doi.org/10.1016/S1470-2045(13)70143-8).
- [7] J.J. Rippey, Why classify basal cell carcinomas? *Histopathology* 32 (1998) 393–398 (accessed August 18, 2018), <http://www.ncbi.nlm.nih.gov/pubmed/9639112>.
- [8] F. Bath-Hextall, M. Ozolins, S.J. Armstrong, G.B. Colver, W. Perkins, P.S.J. Miller, H.C. Williams, Surgery versus Imiquimod for Nodular Superficial basal cell carcinoma (SINS) study group, Surgical excision versus imiquimod 5% cream for nodular and superficial basal-cell carcinoma (SINS): a multicentre, non-inferiority, randomised controlled trial, *Lancet Oncol.* 15 (2014) 96–105, [https://doi.org/10.1016/S1470-2045\(13\)70530-8](https://doi.org/10.1016/S1470-2045(13)70530-8).
- [9] I. Telo, S. Pescina, C. Padula, P. Santi, S. Nicoli, Mechanisms of imiquimod skin penetration, *Int. J. Pharm.* 511 (2016) 516–523, <https://doi.org/10.1016/j.ijpharm.2016.07.043>.
- [10] P. Stein, K. Gogoll, S. Tenzer, H. Schild, S. Stevanovic, P. Langguth, M.P. Radsak, Efficacy of imiquimod-based transcutaneous immunization using a nano-dispersed emulsion gel formulation, *PLoS One* 9 (2014) e102664, <https://doi.org/10.1371/journal.pone.0102664>.
- [11] K. Rehman, M.F.F.M. Aluwi, K. Rullah, L.K. Wai, M.C.I. Mohd Amin, M.H. Zulfakar, Probing the effects of fish oil on the delivery and inflammation-inducing potential of imiquimod, *Int. J. Pharm.* 490 (2015) 131–141, <https://doi.org/10.1016/j.ijpharm.2015.05.045>.
- [12] G.P. Moss, D.R. Gullick, S.C. Wilkinson, *Methods for the measurement of percutaneous absorption*, Predict. Methods Percutaneous Absorpt, Springer Berlin Heidelberg, Berlin, Heidelberg, 2015, pp. 25–42, https://doi.org/10.1007/978-3-662-47371-9_2.
- [13] Y.-C. Kim, J.-H. Park, M.R. Prausnitz, Microneedles for drug and vaccine delivery, *Adv. Drug Deliv. Rev.* 64 (2012) 1547–1568, <https://doi.org/10.1016/J.ADDR.2012.04.005>.
- [14] T.M. Tuan-Mahmood, M.T.C. McCrudden, B.M. Torrisi, E. McAlister, M.J. Garland, T.R.R. Singh, R.F. Donnelly, Microneedles for intradermal and transdermal drug delivery, *Eur. J. Pharm. Sci.* 50 (2013) 623–637, <https://doi.org/10.1016/j.ejps.2013.05.028>.
- [15] K. Van Der Maaden, W. Jiskoot, J. Bouwstra, Microneedle technologies for (trans) dermal drug and vaccine delivery, *J. Control. Release.* 161 (2012) 645–655, <https://doi.org/10.1016/j.jconrel.2012.01.042>.
- [16] R.F. Donnelly, D.I.J. Morrow, P.A. McCarron, A.D. Woolfson, A. Morrissey, P. Juzenas, A. Juzeniene, V. Iani, H.O. McCarthy, J. Moan, Microneedle-mediated intradermal delivery of 5-aminolevulinic acid: potential for enhanced topical photodynamic therapy, *J. Control. Release.* 129 (2008) 154–162, <https://doi.org/10.1016/j.jconrel.2008.05.002>.
- [17] D. Touboul, A. Brunelle, O. Laprèvote, Improvement of biological time-of-flight-secondary ion mass spectrometry imaging with a bismuth cluster ion source, *J. Am. Soc. Mass Spectrom.* 16 (2005) 1608–1618, <https://doi.org/10.1016/j.jasms.2005.06.005>.
- [18] A.M. Judd, D.J. Scurr, J.R. Heylings, K. Wan, P. Gary, Distribution and visualisation of chlorhexidine within the skin using ToF-SIMS: a potential platform for the design of more efficacious skin antiseptic formulations, *Pharm. Res.* 30 (2013) 1896–1905, <https://doi.org/10.1007/s11095-013-1032-5>.
- [19] N.J. Starr, D.J. Johnson, J. Wibawa, I. Marlow, M. Bell, D.A. Barrett, D.J. Scurr, Age-related changes to human stratum corneum lipids detected using time-of-flight secondary ion mass spectrometry following in vivo sampling, *Anal. Chem.* 88 (2016) 4400–4408, <https://doi.org/10.1021/acs.analchem.5b04872>.
- [20] P. Sjövall, T.M. Greve, S.K. Clausen, K. Moller, S. Eirefelt, B. Johansson, K.T. Nielsen, Imaging of distribution of topically applied drug molecules in mouse skin by combination of time-of-flight secondary ion mass spectrometry and scanning electron microscopy, *Anal. Chem.* 86 (2014) 3443–3452, <https://doi.org/10.1021/ac403924w>.
- [21] T. Kezutyte, N. Desbenoit, A. Brunelle, V. Briedis, Studying the penetration of fatty acids into human skin by ex vivo TOF-SIMS imaging, *Biointerphases* 8 (2013) 3, <https://doi.org/10.1186/1559-4106-8-3>.
- [22] V. Čizinauskas, N. Elie, A. Brunelle, V. Briedis, Fatty acids penetration into human skin ex vivo: a TOF-SIMS analysis approach, *Biointerphases* 12 (2017) 011003,

- <https://doi.org/10.1111/1.4977941>.
- [23] V. Čizinauskas, N. Elie, A. Brunelle, V. Briedis, Skin penetration enhancement by natural oils for dihydroquercetin delivery, *Molecules* 22 (2017) 1536, <https://doi.org/10.3390/molecules22091536>.
- [24] F. Benesch-Kieffer, P. Wegrich, R. Schwarzenbach, G. Klecak, T. Weber, J. Leclaire, H. Schaefer, Percutaneous absorption of sunscreens in vitro: interspecies comparison, skin models and reproducibility aspects, *Skin Pharmacol. Physiol.* 13 (2000) 324–335, <https://doi.org/10.1159/000029940>.
- [25] Y.W. Naguib, A. Kumar, Z. Cui, The effect of microneedles on the skin permeability and antitumor activity of topical 5-fluorouracil, *Acta Pharm. Sin. B* 4 (2014) 94–99, <https://doi.org/10.1016/j.apsb.2013.12.013>.
- [26] D.J. Davies, R.J. Ward, J.R. Heylings, Multi-species assessment of electrical resistance as a skin integrity marker for in vitro percutaneous absorption studies, *Toxicol. Vitro* 18 (2004) 351–358, <https://doi.org/10.1016/j.tiv.2003.10.004>.
- [27] L. Bartosova, J. Bajgar, Transdermal drug delivery in vitro using diffusion cells, *Curr. Med. Chem.* 19 (2012) 4671–4677 doi: 1875-533X/12 \$58.00 + .00.
- [28] M.E. Lane, Skin penetration enhancers, *Int. J. Pharm.* 447 (2013) 12–21, <https://doi.org/10.1016/j.ijpharm.2013.02.040>.
- [29] J. Lademann, U. Jacobi, C. Surber, H.-J. Weigmann, J.W. Fluhr, The tape stripping procedure – evaluation of some critical parameters, *Eur. J. Pharm. Biopharm.* 72 (2009) 317–323, <https://doi.org/10.1016/j.ejpb.2008.08.008>.
- [30] S. Fleury, R.F. Vianna Lopez, Topical administration of anticancer drugs for skin cancer treatment, in: *Ski. Cancers – Risk Factors, Prev. Ther., InTech*, 2011. doi: 10.5772/27785.
- [31] L. Anne Skelton, The effective treatment of basal cell carcinoma, *Br. J. Nurs.* 18 (2009) 346–350, <https://doi.org/10.12968/bjon.2009.18.6.40766>.
- [32] H.I. Maibach, Dermal absorption models in toxicology and pharmacology, *Clin. Toxicol.* 45 (2007) 736, <https://doi.org/10.1080/15563650701502766>.
- [33] G.P. Moss, D.R. Gullick, S.C. Wilkinson, Predictive methods in percutaneous absorption, *Predict. Methods Percutaneous Absorpt.* (2015) 1–199, <https://doi.org/10.1007/978-3-662-47371-9>.
- [34] A. Teichmann, S. Heuschkel, U. Jacobi, G. Presse, R.H.H. Neubert, W. Sterry, J. Lademann, Comparison of stratum corneum penetration and localization of a lipophilic model drug applied in an o/w microemulsion and an amphiphilic cream, *Eur. J. Pharm. Biopharm.* 67 (2007) 699–706, <https://doi.org/10.1016/j.ejpb.2007.04.006>.
- [35] E. Chatelain, B. Gabard, C. Surber, Skin penetration and sun protection factor of five UV filters: effect of the vehicle, *Skin Pharmacol. Physiol.* 16 (2003) 28–35, <https://doi.org/10.1159/000068291>.
- [36] K.L. Trebilcock, J.R. Heylings, M.F. Wilks, In vitro tape stripping as a model for in vivo skin stripping, *Toxicol. In Vitro* 8 (1994) 665–667 (accessed August 19, 2018), <http://www.ncbi.nlm.nih.gov/pubmed/20692983>.
- [37] U. Jacobi, H.-J. Weigmann, J. Ulrich, W. Sterry, J. Lademann, Estimation of the relative stratum corneum amount removed by tape stripping, *Ski. Res. Technol.* 11 (2005) 91–96, <https://doi.org/10.1111/j.1600-0846.2005.00094.x>.
- [38] S.J. Bashir, A.L. Chew, A. Anigbogu, F. Dreher, H.I. Maibach, Physical and physiological effects of stratum corneum tape stripping, *Skin Res. Technol.* 7 (2001) 40–48 (accessed August 19, 2018), <http://www.ncbi.nlm.nih.gov/pubmed/11301640>.
- [39] K.M. McKay, B.L. Sambrano, P.S. Fox, R.L. Bassett, S. Chon, V.G. Prieto, Thickness of superficial basal cell carcinoma (sBCC) predicts imiquimod efficacy: a proposal for a thickness-based definition of sBCC, *Br. J. Dermatol.* 169 (2013) 549–554, <https://doi.org/10.1111/bjd.12402>.
- [40] F.J. Verbaan, S.M. Bal, D.J. van den Berg, J.A. Dijkman, M. van Hecke, H. Verpoorten, A. van den Berg, R. Lutge, J.A. Bouwstra, Improved piercing of microneedle arrays in dermatomed human skin by an impact insertion method, *J. Control. Release.* 128 (2008) 80–88, <https://doi.org/10.1016/j.jconrel.2008.02.009>.
- [41] R.E.M. Lutton, J. Moore, E. Larrañeta, S. Ligett, A.D. Woolfson, R.F. Donnelly, Microneedle characterisation: the need for universal acceptance criteria and GMP specifications when moving towards commercialisation, *Drug Deliv. Transl. Res.* 5 (2015) 313–331, <https://doi.org/10.1007/s13346-015-0237-z>.
- [42] S.A. Coulman, J.C. Birchall, A. Alex, M. Pearton, B. Hofer, C. O'Mahony, W. Drexler, B. Považay, In vivo, in situ imaging of microneedle insertion into the skin of human volunteers using optical coherence tomography, *Pharm. Res.* 28 (2011) 66–81, <https://doi.org/10.1007/s11095-010-0167-x>.
- [43] H.G. Kaporis, E. Guttman-yassky, M.A. Lowes, A.S. Haider, J. Fuentes-duculan, K. Darabi, J. Whynot-ertelt, A. Khatcherian, I. Cardinale, I. Novitskaya, G. James, J.A. Carucci, Human basal cell carcinoma is associated with Foxp3⁺T cells in a Th2 dominant microenvironment, *J. Invest. Dermatol.* 127 (2007) 2391–2398, <https://doi.org/10.1038/sj.jid.5700884>.
- [44] Y. Ma, S.E. Boese, Z. Luo, N. Nitin, H.S. Gill, Drug coated microneedles for minimally-invasive treatment of oral carcinomas: development and in vitro evaluation, *Biomed. Microdevices.* 17 (2015), <https://doi.org/10.1007/s10544-015-9944-y>.
- [45] W. Yu, G. Jiang, D. Liu, L. Li, H. Chen, Y. Liu, Q. Huang, Z. Tong, J. Yao, X. Kong, Fabrication of biodegradable composite microneedles based on calcium sulfate and gelatin for transdermal delivery of insulin, *Mater. Sci. Eng. C.* 71 (2017) 725–734, <https://doi.org/10.1016/j.msec.2016.10.063>.